

QCD corrections to top quark spin correlations at hadron colliders *

W. Bernreuther^{†a}, A. Brandenburg^{‡b}, and Z.G. Si^{§a}

^aInstitut f. Theoretische Physik, RWTH Aachen,
D-52056 Aachen, Germany

^bDESY Theory Group, D-22603 Hamburg, Germany

Future hadron collider experiments will allow for a detailed investigation of $t\bar{t}$ spin correlation effects. In this talk, recent progress in the theoretical description of these effects is reported. In particular, next-to-leading order results for the $t\bar{t}$ spin correlations in $q\bar{q} \rightarrow t\bar{t}X$ are presented, using various spin quantization axes.

Top quark pair production and decay can be described by perturbative methods. This is so because the top quark width is large compared to the QCD hadronisation scale and therefore the top decays before hadronisation takes place. The full information of the top quark interactions including spin correlations between t and \bar{t} can thus in principle be obtained from studying differential distributions of the decay products. In this talk, we will report on recent progress in the theoretical description of top quark spin correlation effects at hadron colliders.

Consider the reactions

$$p\bar{p}, pp \rightarrow t\bar{t}X \rightarrow \begin{cases} 2\ell + n \geq 2 \text{ jets} + P_T^{\text{miss}} \\ \ell + n \geq 4 \text{ jets} + P_T^{\text{miss}} \\ n \geq 6 \text{ jets.} \end{cases} \quad (1)$$

To leading order in the QCD coupling, two parton reactions contribute:

$$q\bar{q}, gg \rightarrow t\bar{t} \rightarrow bW^+\bar{b}W^- \rightarrow 6 \text{ fermions.} \quad (2)$$

The amplitudes for these two- to six-body processes, with intermediate top quarks of non-zero total width, were given first in [1]. The calculation of the fully differential cross sections for the reactions (1) including NLO QCD corrections is a formidable task. A substantial simplifi-

cation in the computation of the radiative corrections is achieved if one performs an expansion in Γ_t/m_t and Γ_W/m_W and keeps only the terms with the highest degree of resonance. In this leading pole approximation [2] the radiative corrections can be classified into so-called factorisable and non-factorisable corrections. The non-factorisable NLO QCD corrections were calculated in [3]. For the factorisable corrections the square of the complete matrix element $\mathcal{M}^{(\lambda)}$ for the partonic reactions (2) is of the form

$$|\mathcal{M}^{(\lambda)}|^2 \propto \text{Tr} [\rho R^{(\lambda)} \bar{\rho}] = \rho_{\alpha'\alpha} R_{\alpha\alpha',\beta\beta'}^{(\lambda)} \bar{\rho}_{\beta'\beta}. \quad (3)$$

Here $R^{(\lambda)}$ denotes the density matrix for the production of on-shell $t\bar{t}$ pairs, the label λ indicates the process, and $\rho, \bar{\rho}$ are the density matrices describing the decay of polarised t and \bar{t} quarks, respectively, into specific final states. The subscripts in (3) denote the t, \bar{t} spin indices. Note that both the production and decay density matrices are gauge invariant.

For the process $q\bar{q} \rightarrow t\bar{t}$, which is the dominant process at the Tevatron, the production density matrix R is given in terms of transition matrix elements as follows:

$$R_{\alpha\alpha',\beta\beta'} = \sum_{\substack{\text{colors} \\ q\bar{q} \text{ spins}}} \frac{\langle t_{\alpha}\bar{t}_{\beta} | \mathcal{T} | q\bar{q} \rangle \langle q\bar{q} | \mathcal{T}^\dagger | t_{\alpha'}\bar{t}_{\beta'} \rangle}{N_{q\bar{q}}}, \quad (4)$$

where the factor $N_{q\bar{q}} = (2N_C)^2 = 36$ averages over the spins and colors of the initial $q\bar{q}$ pair. The matrix structure of R is

*Report-no. DESY 00-120

[†]Supported by BMBF contract 05 HT9 PAA 1.

[‡]Speaker at the conference. Supported by a Heisenberg fellowship of D.F.G.

[§]Supported by a A. v. Humboldt fellowship.

$$\begin{aligned}
R_{\alpha\alpha',\beta\beta'} &= A\delta_{\alpha\alpha'}\delta_{\beta\beta'} + C_{ij}(\sigma^i)_{\alpha\alpha'}(\sigma^j)_{\beta\beta'} \\
&+ B_i(\sigma^i)_{\alpha\alpha'}\delta_{\beta\beta'} + \bar{B}_i\delta_{\alpha\alpha'}(\sigma^i)_{\beta\beta'}, \quad (5)
\end{aligned}$$

where σ^i are the Pauli matrices. Using rotational invariance the ‘structure functions’ B_i, \bar{B}_i and C_{ij} can be further decomposed. The function A , which determines the $t\bar{t}$ cross section, is known to next-to-leading order in α_s from the work of [4, 5]. The corresponding function for the gluon fusion process is also known in NLO [4, 6]. Because of parity (P) invariance the vectors $\mathbf{B}, \bar{\mathbf{B}}$ can have, within QCD, only a component normal to the scattering plane. This component, which amounts to a normal polarisation of the t and \bar{t} quarks, is induced by the absorptive part of the scattering amplitude, and it was computed for $q\bar{q}$ and gg initial states in [7, 8] to order α_s^3 . The normal polarisation is quite small, both for $t\bar{t}$ production at the Tevatron and at the LHC. Parity and CP invariance of QCD dictates that the functions C_{ij} , which encode the correlation between the t and \bar{t} spins, have the structure [9]

$$C_{ij} = c_1\delta_{ij} + c_2\hat{p}_i\hat{p}_j + c_3\hat{k}_i\hat{k}_j + c_4(\hat{k}_i\hat{p}_j + \hat{p}_i\hat{k}_j), \quad (6)$$

where $\hat{\mathbf{p}}$ and $\hat{\mathbf{k}}$ are the directions of flight of the initial quark and of the t quark, respectively, in the parton c.m. frame. The production density matrix for the reaction $gg \rightarrow t\bar{t}$ can be defined and decomposed in an analogous fashion. To Born approximation the functions c_r were given, e.g., in [10]. Theoretical studies of spin correlations have been performed at leading order in α_s in [10, 11, 12, 13, 14, 15]. An attempt to detect spin correlations in a small $t\bar{t}$ dilepton sample collected at the Tevatron was recently reported by the D0 collaboration [16]. A feasibility study for the LHC can be found in [17].

We have recently computed the $t\bar{t}$ spin density matrices for the parton reactions $q\bar{q} \rightarrow t\bar{t}, t\bar{t}g$ to order α_s^3 [18]. We have also calculated, for these reactions, the degree of the $t\bar{t}$ spin correlation at NLO for different t and \bar{t} spin quantization axes.

The $t\bar{t}$ spin correlations can be inferred from appropriate angular correlations and distributions of the t and \bar{t} decay products. In the SM the main top decay modes are $t \rightarrow bW \rightarrow bq\bar{q}', b\nu_\ell$.

Among these final states the charged leptons, or the jets from quarks of weak isospin -1/2 originating from W decay, are most sensitive to the polarisation of the top quarks. The one-loop QCD corrections to the semileptonic decays of polarised top quarks and to $t \rightarrow W + b$ can be extracted from the results of [19] and [20, 21], respectively. In the following we describe our computation of the density matrices for $t\bar{t}$ production by $q\bar{q}$ annihilation. At NLO we have to consider the reactions

$$q(p_1) + \bar{q}(p_2) \rightarrow t(k_1) + \bar{t}(k_2), \quad (7)$$

and

$$q(p_1) + \bar{q}(p_2) \rightarrow t(k_1) + \bar{t}(k_2) + g(k_3). \quad (8)$$

In order to determine these functions to order α_s^3 we first computed the one-loop diagrams that contribute to (4). Dimensional regularization was employed to treat both the ultraviolet and the infrared and collinear singularities which appear in the diagrams. The ultraviolet singularities were removed by using the $\overline{\text{MS}}$ prescription for the QCD coupling α_s and the on-shell definition of the top mass m_t . The initial quarks are taken to be massless. After renormalisation the density matrix for the $t\bar{t}$ final state still contains single and double poles in $\epsilon = (4 - D)/2$ due to soft and collinear singularities. These poles are cancelled after including the contributions of the reaction (8) and mass factorization. For the latter we used the $\overline{\text{MS}}$ factorization scheme. We avoided the computation of the exact density matrix for the reaction (8) in D dimensions by employing a simple version of the phase-space slicing method [22]: We divided the phase space into four regions, namely the region where the gluon is soft, the two regions where the gluon is collinear to one of the initial state massless quarks (but not soft), and the complement of these three regions, where all partons are ‘resolved’. This decomposition can be performed using a single dimensionless cut parameter x_{min} . For example, the soft region is defined by the requirement that the scaled gluon energy in the c.m. system $x_g = 2E_g/\sqrt{s}$ is smaller than x_{min} . In the soft region we used the eikonal approximation of the matrix element for reaction (8) and the soft limit of the phase

space measure. The integration over the gluon momentum can then be carried out analytically in D dimensions. The two collinear regions are defined by ($\cos \theta_{qg} > (1 - x_{\min})$ and $x_g > x_{\min}$) and ($\cos \theta_{qg} < (-1 + x_{\min})$ and $x_g > x_{\min}$), respectively, where θ_{qg} is the angle between the gluon and the quark in the $q\bar{q}$ c.m. frame. In these regions we used the collinear approximations for both the squared matrix element and the phase space in D dimensions. Finally, the exact spin density matrix for reaction (8) in four space-time dimensions was used in the resolved region, where all necessary phase space integrations can be carried out numerically. By construction, all four individual contributions depend logarithmically on the slicing parameter x_{\min} , but in the sum only a residual linear dependence on x_{\min} remains, which is due to the approximations made in the soft and collinear regions. By varying x_{\min} between 10^{-3} and 10^{-8} we checked that for $x_{\min} \leq 10^{-4}$ this residual dependence is smaller than our numerical error (which is less than a permill for all results discussed below).

After mass factorisation we are left with finite density matrices for the $t\bar{t}$ and the $t\bar{t}$ + hard gluon final states. As a check of our calculation we first compute the total cross section for $q\bar{q} \rightarrow t\bar{t} + X$ at NLO. If one identifies the $\overline{\text{MS}}$ renormalisation scale μ with the mass factorisation scale μ_F and neglects all quark masses except for m_t , then one can express the cross section in terms of dimensionless scaling functions [4]:

$$\begin{aligned} \hat{\sigma}_{q\bar{q}}(\hat{s}, m_t^2) &= \frac{\alpha_s^2}{m_t^2} [f_{q\bar{q}}^{(0)}(\eta) + 4\pi\alpha_s(f_{q\bar{q}}^{(1)}(\eta) \\ &+ \tilde{f}_{q\bar{q}}^{(1)}(\eta) \ln(\mu^2/m_t^2)], \end{aligned} \quad (9)$$

where \hat{s} is the parton c.m. energy squared and $\eta = \hat{s}/4m_t^2 - 1$. We have compared our result for $\sigma_{q\bar{q}}$ as a function of η with those of [4, 5] and found perfect agreement.

We now consider the following set of spin-correlation observables:

$$\mathcal{O}_1 = 4 \mathbf{s}_1 \cdot \mathbf{s}_2, \quad (10)$$

$$\mathcal{O}_2 = 4 (\hat{\mathbf{k}}_1 \cdot \mathbf{s}_1)(\hat{\mathbf{k}}_2 \cdot \mathbf{s}_2), \quad (11)$$

$$\mathcal{O}_3 = 4 (\hat{\mathbf{p}}_1 \cdot \mathbf{s}_1)(\hat{\mathbf{p}}_1 \cdot \mathbf{s}_2), \quad (12)$$

$$\mathcal{O}_4 = 4 (\hat{\mathbf{p}}_2^* \cdot \mathbf{s}_1)(\hat{\mathbf{p}}_1^{**} \cdot \mathbf{s}_2), \quad (13)$$

$$\mathcal{O}_5 = 4 (\hat{\mathbf{d}}_1 \cdot \mathbf{s}_1)(\hat{\mathbf{d}}_2 \cdot \mathbf{s}_2), \quad (14)$$

where $\mathbf{s}_1, \mathbf{s}_2$ are the t and \bar{t} spin operators, respectively. The factor of 4 is conventional. With this normalization, the expectation value of \mathcal{O}_1 is equal to 1 at the Born level. The expectation values of the observables (11), (12), (13), and (14) determine the correlation of different t, \bar{t} spin projections. Eq. (11) corresponds to a correlation of the t and \bar{t} spins in the helicity basis, while (12) correlates the spins projected along the beam line in the parton c.m.s. The ‘beam-line basis’ used in (13) was defined in [13] and refers to spin axes being parallel to the antiquark direction in the t rest frame $\hat{\mathbf{p}}_2^*$ and to the quark direction in the \bar{t} rest frame $\hat{\mathbf{p}}_1^{**}$, respectively. The spin axes $\hat{\mathbf{d}}_{1,2}$ in (11) correspond to the so-called ‘optimal basis’ [23, 14] to be discussed below.

For quark-antiquark annihilation it turns out that the spin correlation (12) [10, 15] and the correlation in the beam-line basis (13) [13] are stronger than the correlation in the helicity basis. A spin-quantization axis was constructed in [23, 14] with respect to which the t and \bar{t} spins are 100% correlated to leading order in the QCD coupling, for all energies and scattering angles. In terms of the structure functions of (5) this means that the ‘optimal’ spin axis $\hat{\mathbf{d}}$ fulfills the condition

$$\hat{d}_i C_{ij} \hat{d}_j = A. \quad (15)$$

The existence of a solution of Eq. (15) is a special property of the leading order spin density matrix for the reaction $q\bar{q} \rightarrow t\bar{t}$. One finds [23, 14]:

$$\hat{\mathbf{d}} = \frac{-\hat{\mathbf{p}}_1 + (1 - \gamma_1)(\hat{\mathbf{p}}_1 \cdot \hat{\mathbf{k}}_1)\hat{\mathbf{k}}_1}{\sqrt{1 - (\hat{\mathbf{p}}_1 \cdot \hat{\mathbf{k}}_1)^2(1 - \gamma_1^2)}}, \quad (16)$$

where $\gamma_1 = E_1/m_t$. The construction of this axis explicitly uses the leading order result for the spin density matrix, and different generalizations to higher orders are possible. We use in (14) as spin axes:

$$\begin{aligned} \hat{\mathbf{d}}_1 &= \hat{\mathbf{d}}, \\ \hat{\mathbf{d}}_2 &= \frac{-\hat{\mathbf{p}}_1 + (1 - \gamma_2)(\hat{\mathbf{p}}_1 \cdot \hat{\mathbf{k}}_2)\hat{\mathbf{k}}_2}{\sqrt{1 - (\hat{\mathbf{p}}_1 \cdot \hat{\mathbf{k}}_2)^2(1 - \gamma_2^2)}}, \end{aligned} \quad (17)$$

where $\gamma_2 = E_2/m_t$. For the 2 to 2 process $q\bar{q} \rightarrow t\bar{t}$, $\hat{\mathbf{d}}_2 = \hat{\mathbf{d}}_1 = \hat{\mathbf{d}}$.

The expectation value of a spin-correlation observable \mathcal{O} at parton level can be written at next-to-leading order in analogy to (9) as follows:

$$\begin{aligned} \langle \mathcal{O} \rangle_{q\bar{q}} &= g_{q\bar{q}}^{(0)}(\eta) + 4\pi\alpha_s(g_{q\bar{q}}^{(1)}(\eta) \\ &+ \tilde{g}_{q\bar{q}}^{(1)}(\eta) \ln(\mu_F^2/m_t^2)). \end{aligned} \quad (18)$$

Note that these quantities depend explicitly on the factorization scale μ_F , but only implicitly (through α_s) on the renormalization scale μ . This is because a factor α_s^2 drops out in the expectation values, and hence the Born result is of order α_s^0 .

Our results for the functions $g_{q\bar{q}}^{(0)}(\eta)$, $g_{q\bar{q}}^{(1)}(\eta)$ and $\tilde{g}_{q\bar{q}}^{(1)}(\eta)$ are shown for the five observables (10)-(14) in Figs. 1-5. In each figure, the dotted line is the Born result $g_{q\bar{q}}^{(0)}(\eta)$, the full line shows the function $g_{q\bar{q}}^{(1)}(\eta)$, and the dashed line is $\tilde{g}_{q\bar{q}}^{(1)}(\eta)$. A general feature of all results is that the QCD corrections are very small for values of $\eta \lesssim 1$. For larger values of η , the functions $g_{q\bar{q}}^{(1)}(\eta)$ depart significantly from zero. Also, the functions $\tilde{g}_{q\bar{q}}^{(1)}(\eta)$ become nonzero, with less dramatic growth as $\eta \rightarrow \infty$ and with an opposite sign as compared to $g_{q\bar{q}}^{(1)}(\eta)$. The phenomenological implications of these features for spin correlations at the Tevatron and the LHC will be studied in detail in a future work. Here we merely note that the substantial QCD corrections for large η will be damped by the parton distribution functions, which decrease rapidly with η . Moreover, at Tevatron energies values of η above ~ 30 are kinematically excluded.

To summarize: We have computed the spin density matrices describing $t\bar{t}$ production by $q\bar{q}$ annihilation to order α_s^3 . Further we have evaluated the scaling functions encoding the QCD corrections to spin correlations, using a number of different spin quantization axes. This work provides a building block, which was missing so far, towards a complete description of the hadronic production of top quark pairs at NLO in the strong coupling.

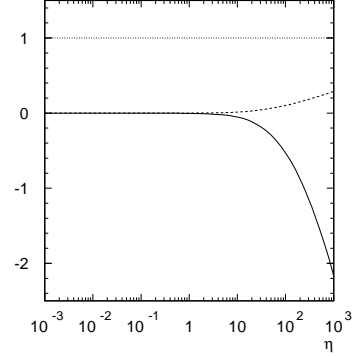


Figure 1. Dimensionless scaling functions $g_{q\bar{q}}^{(0)}(\eta)$ (dotted), $g_{q\bar{q}}^{(1)}(\eta)$ (full), and $\tilde{g}_{q\bar{q}}^{(1)}(\eta)$ (dashed) that determine the expectation value $\langle \mathcal{O}_1 \rangle_{q\bar{q}}$.

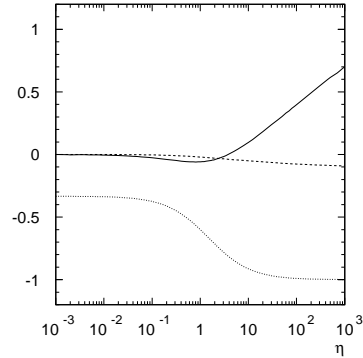


Figure 2. Same as Fig.1, but for $\langle \mathcal{O}_2 \rangle_{q\bar{q}}$.

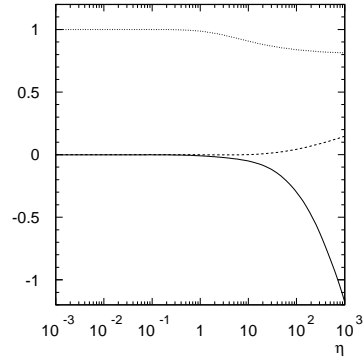


Figure 3. Same as Fig.1, but for $\langle \mathcal{O}_3 \rangle_{q\bar{q}}$.

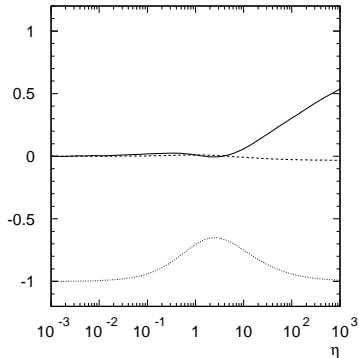


Figure 4. Same as Fig.1, but for $\langle \mathcal{O}_4 \rangle_{q\bar{q}}$.

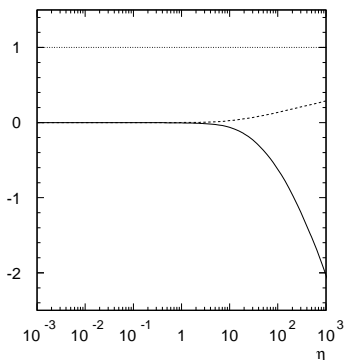


Figure 5. Same as Fig.1, but for $\langle \mathcal{O}_5 \rangle_{q\bar{q}}$.

REFERENCES

1. R. Kleiss and W. J. Stirling, Z. Phys. C 40 (1988) 419.
2. R. G. Stuart, Phys. Lett. B 262 (1991) 113; A. Aeppli, G. J. van Oldenborgh and D. Wyler, Nucl. Phys. B 428 (1994) 126.
3. W. Beenakker, F. A. Berends and A. P. Chapovsky, Phys. Lett. B 454 (1999) 129.
4. P. Nason, S. Dawson and R. K. Ellis, Nucl. Phys. B 303 (1988) 607; Nucl. Phys. B 327 (1989) 49.
5. W. Beenakker, W. L. van Neerven, R. Meng, G. A. Schuler and J. Smith, Nucl. Phys. B 351 (1991) 507.
6. W. Beenakker, H. Kuijf, W. L. van Neerven and J. Smith, Phys. Rev. D 40 (1989) 54.
7. W. Bernreuther, A. Brandenburg and P. Uwer, Phys. Lett. B 368 (1996) 153.
8. W. G. Dharmaratna and G. R. Goldstein, Phys. Rev. D 53 (1996) 1073.
9. W. Bernreuther and A. Brandenburg, Phys. Rev. D 49 (1994) 4481.
10. A. Brandenburg, Phys. Lett. B 388 (1996) 626.
11. V. Barger, J. Ohnemus and R. J. Phillips, Int. J. Mod. Phys. A 4 (1989) 617.
12. T. Stelzer and S. Willenbrock, Phys. Lett. B 374 (1996) 169.
13. G. Mahlon and S. Parke, Phys. Rev. D 53 (1996) 4886.
14. G. Mahlon and S. Parke, Phys. Lett. B 411 (1997) 173.
15. D. Chang, S. Lee and A. Sumarokov, Phys. Rev. Lett. 77 (1996) 1218.
16. B. Abbott *et al.* (D0 Collaboration), Phys.Rev.Lett. 85 (2000) 256.
17. M. Beneke *et. al.*, "Top Quark Physics" in: Report of the "1999 CERN Workshop on SM physics (and more) at the LHC", hep-ph/0003033.
18. W. Bernreuther, A. Brandenburg and Z.G. Si, Phys.Lett. B483 (2000) 99.
19. A. Czarnecki, M. Jezabek and J. H. Kühn, Nucl. Phys. B 351 (1991) 70.
20. C. R. Schmidt, Phys. Rev. D 54 (1996) 3250.
21. M. Fischer, S. Groote, J. G. Körner, M. C. Mauser and B. Lampe, Phys. Lett. B 451 (1999) 406.
22. W. T. Giele, E. W. N. Glover and D. A. Kosower, Nucl. Phys. B 403 (1993) 633.
23. S. Parke and Y. Shadmi, Phys. Lett. B 387 (1996) 199.

Discussion

A.P. Contogouris, Univ. of Athens

I am worried not by the method of your calculation, but by the importance of your numerical results. In particular the channel $gg \rightarrow t\bar{t}(g)$ can change them very much, and I am glad that you have already set up its calculation. Of course, $q\bar{q} \rightarrow t\bar{t}(g)$ is required to be complete.

A. Brandenburg

I agree. Note that the plots show results at the parton level for $q\bar{q} \rightarrow t\bar{t}(g)$.